Fuel 234 (2018) 110–119

Contents lists available at ScienceDirect

Fuel

journal homepage: www.elsevier.com/locate/fuel

Full Length Article

Modified Ag/TiO_2 systems: Promising catalysts for liquid-phase oxidation of alcohols

E. Kolobova[a,*], Y. Kotolevich[b], E. Pakrieva[a], G. Mamontov[c], M.H. Farias[b], V. Cortés Corberán[d], N. Bogdanchikova[b], J. Hemming[e], A. Smeds[e], P. Mäki-Arvela[e], D. Yu. Murzin[e], A. Pestryakov[a]

[a] Tomsk Polytechnic University, Tomsk 634050, Russia
[b] Centro de Nanociencias y Nanotecnología, Universidad Nacional Autónoma de México, Ensenada 22860, Mexico
[c] Tomsk State University, Tomsk 634050, Russia
[d] Institute of Catalysis and Petroleumchemistry (ICP), Spanish Council for Scientific Research (CSIC), 28049 Madrid, Spain
[e] Johan Gadolin Process Chemistry Centre, Abo Akademi University, FI-20500 Turku, Finland

GRAPHICAL ABSTRACT

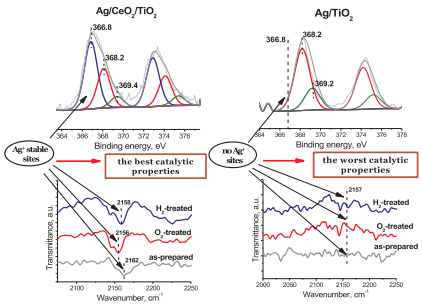

ARTICLE INFO

Keywords:
n-Octanol oxidation
Betulin oxidation
Alcohols selective oxidation
Silver catalysts
Silver active sites
Support modifiers
Effect of redox pretreatment

ABSTRACT

The current work is the first study concerning the liquid-phase oxidation of n-octanol and betulin over modified and unmodified Ag/TiO_2 catalysts. Catalytic activity of nanosilver catalysts supported on titania for alcohols selective oxidation can be enhanced by modification of the support with Ce, Fe or Mg oxides. In most cases reductive or oxidative pretreatments of these catalysts were detrimental for their activity. The main reason for performance of $Ag/M_xO_y/TiO_2$ catalysts is changes of the electronic state of the supported Ag, and especially changes in the surface concentration of Ag^+ ions. Monovalent Ag^+ ions are active sites in silver-containing catalysts for n-octanol, as well as for betulin oxidation. The obtained results show a potential of silver-containing catalysts for liquid phase oxidation of alcohols, and by selecting the optimum modifier and the support as well as, pretreatment conditions the catalytic properties and stabilization of the active sites can be optimized.

1. Introduction

Development of sustainable chemical processes implies utilization of renewable feedstocks and design for energy efficiency, conducting them under the lowest pressure and temperature, avoiding if possible the use of auxiliary substances, adhering to the principles of atom economy, and preventing wastes and a negative environmental impact. Selective oxidation of alcohols is one of the key transformations in organic synthesis and in industrial practice, with a global annual production of carbonyl compounds of 10,000 million t/yr at the end of

* Corresponding author.
E-mail address: ekaterina_kolobova@mail.ru (E. Kolobova).

https://doi.org/10.1016/j.fuel.2018.06.128
Received 14 March 2018; Received in revised form 5 June 2018; Accepted 29 June 2018
Available online 10 July 2018
0016-2361/

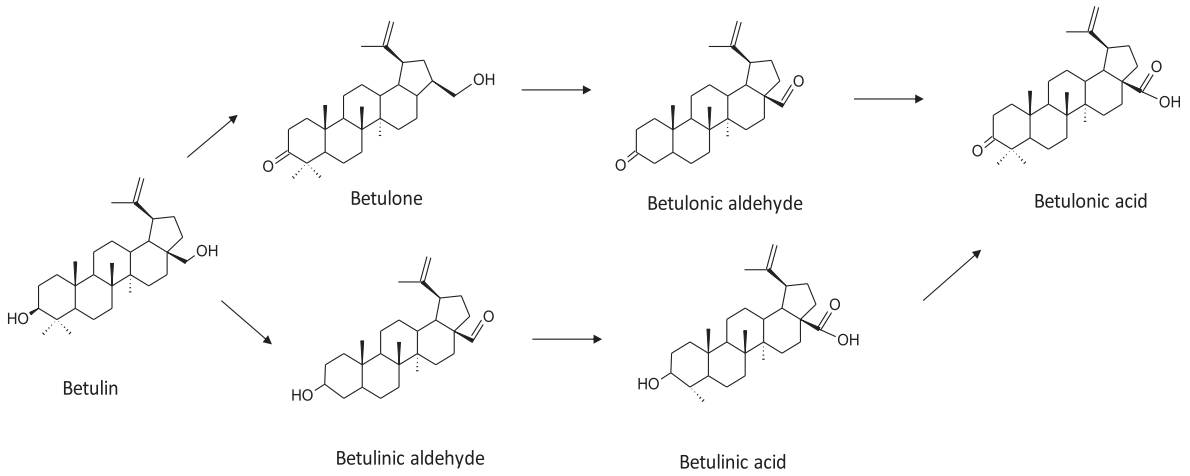

Scheme 1. Reaction scheme for betulin oxidation.

20th century [1]. Currently most of industrial alcohol oxidation processes are based on the use of stoichiometric oxidizing agents and/or alkalis, and thus are not environmentally friendly. Catalytic oxidation processes have opened up a possibility of obtaining carbonylic compounds using oxidizing agents such as air or oxygen. In particular, catalysts based on noble metal nanoparticles have allowed approaching the aforementioned sustainability criteria, due to their extraordinary activity under very mild reaction conditions.

Linear primary alkanols are the least reactive for oxidation type of alcohols, with their reactivity decreasing with an increase of the carbon chain. This makes n-octanol a convenient model compound for comparative studies of catalysts for oxidation of alcohols [2]. Since n-octanol is more difficult to oxidize than most commercially important alcohols, catalysts active in its oxidation will be more effective in similar processes.

Nanogold catalysts are frequently used in the literature for selective oxidation of alcohols [3,4], however, their drawbacks include: high cost and fast deactivation during reaction or after prolonged storage [5]. As an alternative, catalytic systems based on silver exhibit lower activity than supported gold in a number of processes, being more active compared with many oxide and metal catalysts, they are much more stable and cheaper than gold-containing systems. Despite this, there are less than 20 papers devoted to liquid-phase oxidation of alcohols on silver catalysts [6–21]. This is surprising, as silver catalysts are excellent in gas-phase oxidations such as epoxidation of ethylene [22], synthesis of formaldehyde [23], neutralization of NO_x [24], selective oxidation of ammonia [25], gas-phase partial oxidation of benzyl alcohol [26], oxidative coupling of methane [27], oxidation of styrene [28], selective oxidation of ethylene glycol [29], CO oxidation [30–33], etc.

Nevertheless, and despite a small number of studies devoted to liquid-phase selective oxidation of alcohols using silver-containing catalysts, it is obvious that these systems have a potential in such processes, being able to replace existing expensive catalysts based on platinum-group metals and gold.

To the best of our knowledge only two papers devoted to n-octanol oxidation using silver catalysts were published [6,15]. Wang et al. [6] proposed a method of selective liquid-phase oxidation of benzyl and allyl alcohols in the presence of sodium carbonate using $AgNO_3$ (2 mol. %) as a catalyst in the presence of Na_2CO_3 (2 mmol), and air as an oxidant. The main disadvantage of their approach is the use of sodium carbonate, which leads to formation of undesired by-products and waste. The second important drawback is the complexity of extracting the catalytic system from the reaction medium and impossibility of its reuse. Beier et al. [15] investigated activity of a number of silver catalysts supported on SiO_2, Al_2O_3, celite, CeO_2, kaolin, MgO, and activated carbon in the selective liquid-phase oxidation of different alcohols (including oxidation of n-octanol) using a special screening approach: five to six catalyst samples were mixed and tested simultaneously. Thereby, a synergetic effect between ceria nanoparticles and silver-impregnated silica (10 wt% Ag–SiO_2) was found using a physical mixture of them. The catalytic activity was strongly dependent on the silver loading, the amount of ceria, and especially the calcination procedure. In addition, presence of ceria increased catalytic activity of all investigated catalysts. However, despite a rather high activity (for example, n-octanol conversion after 45 min was 29%), this process was carried out at a sufficiently high pressures (2.5–5.0 MPa) and temperatures (100–200 °C). In addition, reuse of the catalyst led to a decrease of alcohol conversion from 98% to 16%, which is a very significant disadvantage.

On the current work feasibility of using nanosilver catalysts to oxidize selectively less reactive alcohols, such as n-octanol, was elucidated under conditions close to the requirements of “green chemistry”: atmospheric pressure, a non-toxic solvent, no alkaline additives and initiators, and a relatively low temperature.

In the present work for comparison Ag-containing catalysts were applied for liquid phase oxidation of betulin (lup-20(29)-ene-3,28-diol, $C_{30}H_{50}O_2$, CAS: 473-98-3) – pentacyclic triterpenoide of lupane series, which is present in the bark of some tree species, such as *Betula* sp. [34,35]. Betulin, and especially its oxo-derivatives (betulone, betulinic and betulonic aldehydes, betulinic and betulonic acids, as well as their derivatives) have valuable biologically active properties (for example, exhibit a multitude of pharmacological properties ranging from antitumor, antiinflammatory, antiparasitic, anti-HIV activities, etc.) and are of exceptional interest for the pharmaceutical, cosmetic and food industries [36,37]. The reaction scheme for betulin oxidation is shown in Scheme 1. In nowadays, the main method of synthesis of betulin oxo-derivatives is by oxidation. The most commonly used oxidants are Cr (VI) compounds in a strongly acidic medium, for example, the Jones’s reagent [36]. However, despite numerous studies aimed at modifying the method of betulin oxidation by the Jones’s reagent, production of oxo-derivatives is rather complex and challenging being characterized by a low yield of the target products (50–65%), low temperature (− 5 °C to 10 °C) and duration of the synthesis (up to 24 h), low selectivity leading to a mixture of products, as well as complexity of toxic Cr(III) utilization and very toxic residual of Cr(VI). Accordingly, extraction of a pure product requires complex purification, a use of a large number of different types of organic solvents and various methods for utilization Cr(III). Besides chemical modifications, several attempts of biological transformation of betulin by means of microorganisms were undertaken [38]. However, biotransformations of betulin using opportunistic yeast, fungi, etc. have significant drawbacks, since they require complex

nutrient media, a long duration, a low conversion level when low concentrations of the starting compound are introduced. There is only one paper devoted to the liquid phase oxidation of betulin using Pd and Ru supported on different supports as heterogeneous catalysts [39]. The authors [39] the first demonstrated the selective oxidation of betulin to betulinic aldehyde over Ru/C catalyst mixed with basic hydrotalcite and SiO_2 as dehydrating agent in synthetic air at 108 °C in toluene with conversion of 41% in 24 h and 67% selectivity to betulinic aldehyde, whereas without SiO_2 with Ru/C the corresponding conversion and selectivity values were 20% and 66%, respectively. Over another, acidic Ru/C catalyst even higher conversion was achieved, giving, however, allobetulin as a main product. Thus, there is a clear need to develop new methods and approaches to produce oxo-derivatives of betulin, which would replace the existing stoichiometric processes leading to formation of a large amount of toxic waste, but at the same time provide a quantitative yield of the target product.

The aim of the present study is to evaluate a perspective of using silver-based catalysts in the liquid phase selective oxidation of n-octanol, to estimate influence of Mg, Fe and Ce oxides as additives and redox pretreatments on catalytic properties and to elucidate the nature of the active sites. The obtained results were compared with catalytic behaviour of the catalysts in betulin oxidation which has high importance in drug production.

2. Experimental

2.1. Catalysts preparation

Titania P25 from Evonik ($45\ m^2g^{-1}$, nonporous, 70% anatase and 30% rutile, purity > 99.5%) was used as a starting support. $Ce(NO_3)_3{\cdot}6H_2O$, $Fe(NO_3)_3{\cdot}9H_2O$ and $Mg(NO_3)_2{\cdot}6H_2O$ (Aldrich) were used as modifier (M) precursors and $AgNO_3$ (Aldrich) as a silver precursor.

Prior to any use, TiO_2 was dried in air at 100 °C for at least 24 h. Modified supports with a molar ratio Ti/M = 40 were prepared by impregnation of the initial TiO_2 with 2.5 cm^3/g of aqueous solutions of the corresponding nitrates. The impregnated supports were dried at room temperature for 48 h, then at 110 °C for 4 h and finally calcined at 550 °C for 4 h.

Ag/TiO_2 and $Ag/M_xO_y/TiO_2$ (M = Ce, Fe, Mg) catalysts with 2.3 wt % Ag nominal loading were prepared by deposition-precipitation with NaOH in the absence of light. To 54 ml of an aqueous solution containing $AgNO_3$ (4.2×10^{-3} M), 1 g of TiO_2 was added, thereafter the mixture was heated to 80 °C, the initial pH was ~3 followed by pH adjustment to 9 by adding dropwise a solution of NaOH (0.5 M). The suspension was kept at 80 °C for 2 h under vigorous stirring.

After precipitation, all samples were centrifuged, washed four times with 100 ml of distilled water followed by centrifugation then dried under vacuum for 2 h at 80 °C. After preparation, the samples were stored at room temperature in a desiccator under vacuum, in a place protected from light.

2.2. Catalysts characterization

Temperature-programmed reduction with hydrogen (H_2 TPR) was performed in a fixed-bed quartz reactor with a Micromeritics AutoChem 2950 analyzer, by a heating at a rate of $10\ °C{\cdot}min^{-1}$ from 25 up to 900 °C under a flow of $20\ cm^3{\cdot}min^{-1}$ of 10 vol% H_2/Ar reducing mixture. Hydrogen consumption was measured by thermal conductivity detector. The trap with of liquid nitrogen and isopropanol (~ −90 °C) was used to condense water. Ag_2O (Micromeritics) was used as a standard for calibrating the amount of hydrogen consumed. The catalysts were studied by H_2 TPR either as-prepared and after redox pretreatments at 300 °C for 30 min: oxidative in flow of $20\ cm^3{\cdot}min^{-1}$ air or reductive in flow of H_2/Ar gas mixture.

Fourier transform infrared (FTIR) spectra of CO adsorbed on the catalysts were recorded by using a Bruker Tensor 27 FTIR spectrometer in transmittance mode with $4\ cm^{-1}$ resolution. *In situ* experiments were carried out in a quartz cell with NaCl windows. The sample powder was pressed into disks of 13 mm diameter and ~20 mg weight. For each catalyst three samples were investigated: as-prepared, and after pretreatments either in H_2 or in O_2 (100 Torr) at 300 °C for 1 h and then cooled down for room temperature. Thereafter, H_2 or O_2 was evacuated and CO adsorption (Matheson Research grade, P_0 = 30 Torr) was carried out. CO spectra presented in this work were obtained by subtracting the gas phase CO spectrum.

Due to conditions of equipment utilization, prior any other characterization the samples were pretreated in hydrogen at 300 °C for 1 h.

Textural properties of catalysts and supports were determined from nitrogen adsorption-desorption isotherms (−196 °C) recorded with a Micromeritics TriStar 3000 apparatus. Prior to experiments, the samples were degassed at 300 °C in vacuum for 5 h. The adsorbed N_2 volume was normalized to standard temperature and pressure. The specific surface areas (S_{BET}) of the samples were calculated by applying the BET method to the nitrogen adsorption data within the P/P_0 range 0.05–0.25.

X-ray powder diffraction was conducted by the step-scanning procedure (step size 0.02°; 0.5 s) with a Philips XPert PRO diffractometer, using Ni-filtered CuKα (λ = 0.15406 nm) radiation. Assignment of crystalline phases was based on the ICDD-2013 powder diffraction database.

High resolution transmission electron microscopy (HR TEM) studies were carried out using a JEOL JEM-2100F microscope operating with a 200 kV accelerating voltage. The samples were ground into a fine powder and dispersed ultrasonically in hexane at room temperature. Then, a drop of the suspension was put on a lacey carbon-coated Cu grid. At least ten representative images were taken for each sample. A particle size distribution was obtained by counting at least 100 particles for each sample. Silver contents were measured by energy dispersive spectroscopy (EDS) in the same system equipped with a Kevex Superdry detector. Elemental mapping was carried out by EDS with an X-Max device from Oxford Instruments.

The samples were characterized by X-ray photoelectron spectroscopy (XPS) with a SPECS GmbH custom made system using a PHOIBOS 150 WAL hemispherical analyzer and a non-monochromated X-ray source. All the data were acquired using Al Kα X-rays (1486.6 eV, 200 W). A pass-energy of 50 eV, a step size of 0.1 eV/step and a high-intensity lens mode were selected. The diameter of the analysed area was 3 mm. Charging shifts were referenced against the Ti $2p_{3/2}$ peak of TiO_2 at 458.8 eV. The pressure in the analysis chamber was kept lower than 1×10^{-8} mbar. The accuracy of the binding energy (BE) values was ± 0.1 eV. Spectra are presented without smoothing or background subtraction, with intensity expressed in counts-per-second (cps). Peak areas were estimated by calculating the integral of each peak after subtracting a Shirley type background, fitting the experimental peak to a combination of Lorentzian/Gaussian lines with a 30/70 proportion and keeping the same width on all lines.

2.3. Catalytic testing

Catalytic measurements for n-octanol oxidation were performed with samples either as-prepared or after being treated in pure hydrogen flow or in pure oxygen flow at 300 °C for 1 h. Typically, a supported silver catalyst was added in a substrate/metal ratio = 100 mol/mol to 20 ml of n-octanol substrate (0.1 M) (Sigma Aldrich 99%, HPLC grade) in n-heptane (Scharlau, 99%, HPLC grade) as a solvent, in a four-necked round bottom flask equipped with a reflux condenser, an oxygen feeded, a thermometer and a septum cap. The reaction mixture was stirred (200 rpm) in a semibatch reactor operated under atmospheric pressure at 80 °C. Oxygen (30 ml/min) (Air Liquide, 99.99%) was bubbled through the suspension and the reaction was followed for 6 h. Small aliquots of the reaction mixture were taken during and at the end of the test, by using nylon syringe filters (pore 0.45 μm), for monitoring

progress of the reaction. Reactants and products were analysed in a Varian 450 gas chromatograph, using a capillary DB wax column (15 m × 0.548 mm) and He as the carrier gas. The temperature program was as follows: oven: starting temperature 100 °C, 0.1 min initial hold, heating rate 30 °C/min, final temperature 220 °C, 1.9 min hold; injector: 220 °C; FID detector: 200 °C, both isothermal.

Betulin (90–94%) was extracted from birch with a non-polar solvent and recrystallized from 2-propanol following the procedure described previously in [40]. Betulin oxidation was performed over as-prepared modified and unmodified Ag/TiO_2 catalysts at 140 °C under atmospheric pressure with synthetic air (AGA, 20% oxygen, 80% nitrogen) as an oxidant in mesitylene (Sigma Aldrich, > 99%). Typically oxidation of betulin was carried out using 200 mg of the reagent in 100 ml of the solvent using 200 mg of the catalyst. The reaction was commenced when the desired temperature was reached via turning on the stirring (400 rpm). The samples for analysis were withdrawn from the reactor at regular intervals. Prior to GC-analyses, the samples (150 μL) were silylated by adding 150 μL of a mixture of pyridine (VWR International, Fontenay-sous-Bois, France), N,O-bis(trimethylsilyl)trifluoroacetamide (BSTFA, Supelco Analytical, Bellefonte, PA, USA), and trimethylsilyl chloride (TMCS, Merck KGaA, Darmstadt, Germany) in a 1:4:1 vol ratio, and the mixture was heated in an oven at 70 °C for 45 min. GC analysis was performed on a PerkinElmer AutosystemXL gas chromatograph using an Agilent HP-1 capillary column, 25 m (L) × 0.2 mm (ID), film thickness 0.11 mm. Hydrogen was used as a carrier gas, with a flow of 0.8 ml/min. The temperature programs were as follows: oven – starting temperature 120 °C, 1 min initial hold, increase at 6 °C/min rate to the final temperature 320 °C, 15 min hold; injector – 160 °C, (0 min), 8 °C/min to 260 °C, 15 min hold; FID detector –- 320 °C isotermal. The injection volume was 1 μL with a split ratio 24:1. Betulinic aldehyde and betulinic acid (90% purity), used as standards, were purchased from MedChem Express and Sigma Aldrich, respectively. Betulonic aldehyde and acid were synthesized according to the method reported by Melnikova et al. [41] in acetone (Sigma Aldrich, > 99.9) at 25 °C using potassium dichromate, $K_2Cr_2O_7$ (Merck, 99.8%) as an oxidant and sulphuric acid as a catalyst. The products were confirmed by GC–MS with HP-5 column. The conditions of the betulin oxidation process and the analysis procedure were previously published in [36]. Differences in the experimental conditions for oxidation of n-octanol and betulin are related to different solubility of these alcohols.

3. Results and discussion

Fig. 1 shows the effect of the support nature and catalyst pretreatment on n-octanol conversion (Fig. 1a) and product distribution (Fig. 1b) in n-octanol oxidation over as-prepared samples and after each of the redox treatments. It should be noted that, in the as-prepared state (red line in Fig. 1) all used additives exert a promotional effect on octanol oxidation over Ag/TiO_2 increasing its activity up to fourfold in the case of modification by Ce. Both redox pretreatments decreased activity of all studied catalysts in n-octanol oxidation except prereduction of $Ag/MgO/TiO_2$ with H_2 which had no effect; the as-prepared samples were the most active.

Aldehyde, octanal, was the main product of n-octanol oxidation on all as-prepared catalysts (Fig. 1b) with selectivity above 90% after 6 h of reaction. Only traces of octanoic acid and the ester, octyl octanoate, were detected at the longest reaction times.

To assess a possibility of using Ag-containing catalysts in the liquid phase oxidation of betulin and to carry out comparative studies, Ag/TiO_2 and $Ag/CeO_2/TiO_2$ were chosen based on the results with n-octanol. In betulin oxidation (Fig. 2a) modification by ceria improved the catalytic properties, similar to n-octanol oxidation. Conversion of betulin over this catalyst reached 27% after 6 h which was substantially larger than 11% obtained for Ag/TiO_2. In all cases the main reaction product was betulone with selectivity > 60% (Fig. 2b, c). The second and third largest reaction products in the case of $Ag/CeO_2/TiO_2$ were

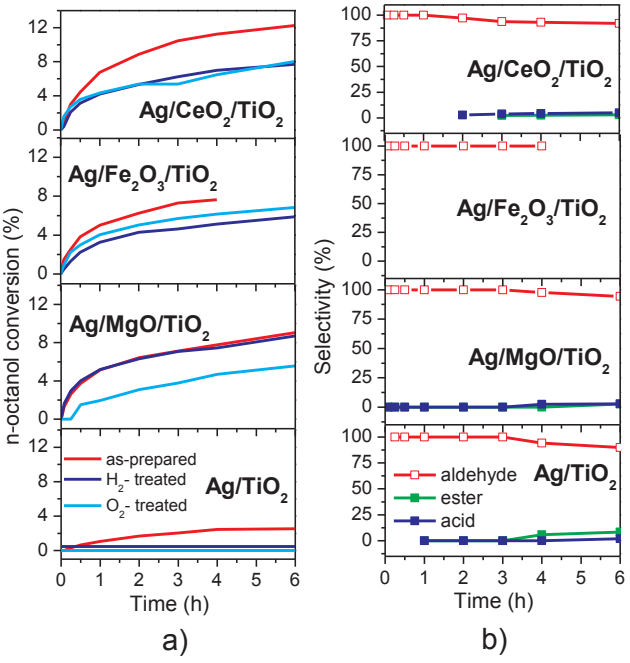

Fig. 1. Effect of the support nature and pretreatment on the catalytic properties in oxidation of 1-octanol (a) over supported Ag catalysts: as-prepared (red), treated in flow of H_2 (dark-blue) or O_2 (light-blue) at 300 °C for 1 h. Selectivity of products in n-octanol oxidation for as-prepared samples (b). (For interpretation of the references to colour in this figure legend, the reader is referred to the web version of this article.)

betulinic aldehyde and betulinic acid (6% and 7%, respectively). In the case of the unmodified catalyst, these products were betulinic and betulonic aldehydes (22% and 8%, respectively). Comparing the results of current work with previously published in [39] it can be concluded that silver-containing catalysts are perspective for liquid phase oxidation of betulin. However, they require further improvement.

Kinetic curves in betulin oxidation for the cerium-modified and unmodified catalysts were very different (Fig. 2), $Ag/CeO_2/TiO_2$ was much more active. On the contrary for Ag/TiO_2 catalytic activity declined substantially. The results are in line with n-octanol oxidation (Fig. 1a), when the cerium-modified catalyst was more active than the parent material. Certainly, the operating conditions in both processes are different (for example, temperature, solvent), as well as physicochemical properties of the substrates (alcohols), primarily solubility. However, general trends in the catalytic behaviour are similar.

To determine the reasons for these differences in the catalytic behaviour among the studied catalysts, several physical and chemical characterization methods were applied.

To study the phase composition of the investigated catalysts XRD was used (data not shown). Analysis of diffractograms showed absence of reflexes characteristic for silver and modifiers, implying that silver particles and modifiers are smaller than 3–4 nm (i.e. sensitivity threshold of XRD) or they are X-ray amorphous. This was also confirmed by XRD-SR data published in [33], where the reflections corresponding to the modifier were only detected for $Ag/CeO_2/TiO_2$.

The specific surface areas of the modified supports and the catalysts are rather close, and the content of Ag was almost the same for all catalysts (Table 1). Thus, the textural properties and silver content cannot be the reason for different catalytic behaviour.

Table 1 also shows the metal particle size data for $Ag/CeO_2/TiO_2$, $Ag/Fe_2O_3/TiO_2$, and $Ag/MgO/TiO_2$ reported previously in [33]. As can be seen, these three catalysts display very different range and average values of silver particle sizes (7.2, 1.1 and 5.5 nm, respectively). However, our previous study based on comparison of XRD-SR, HR TEM, EDS and DRS data showed that the majority of silver particles on these

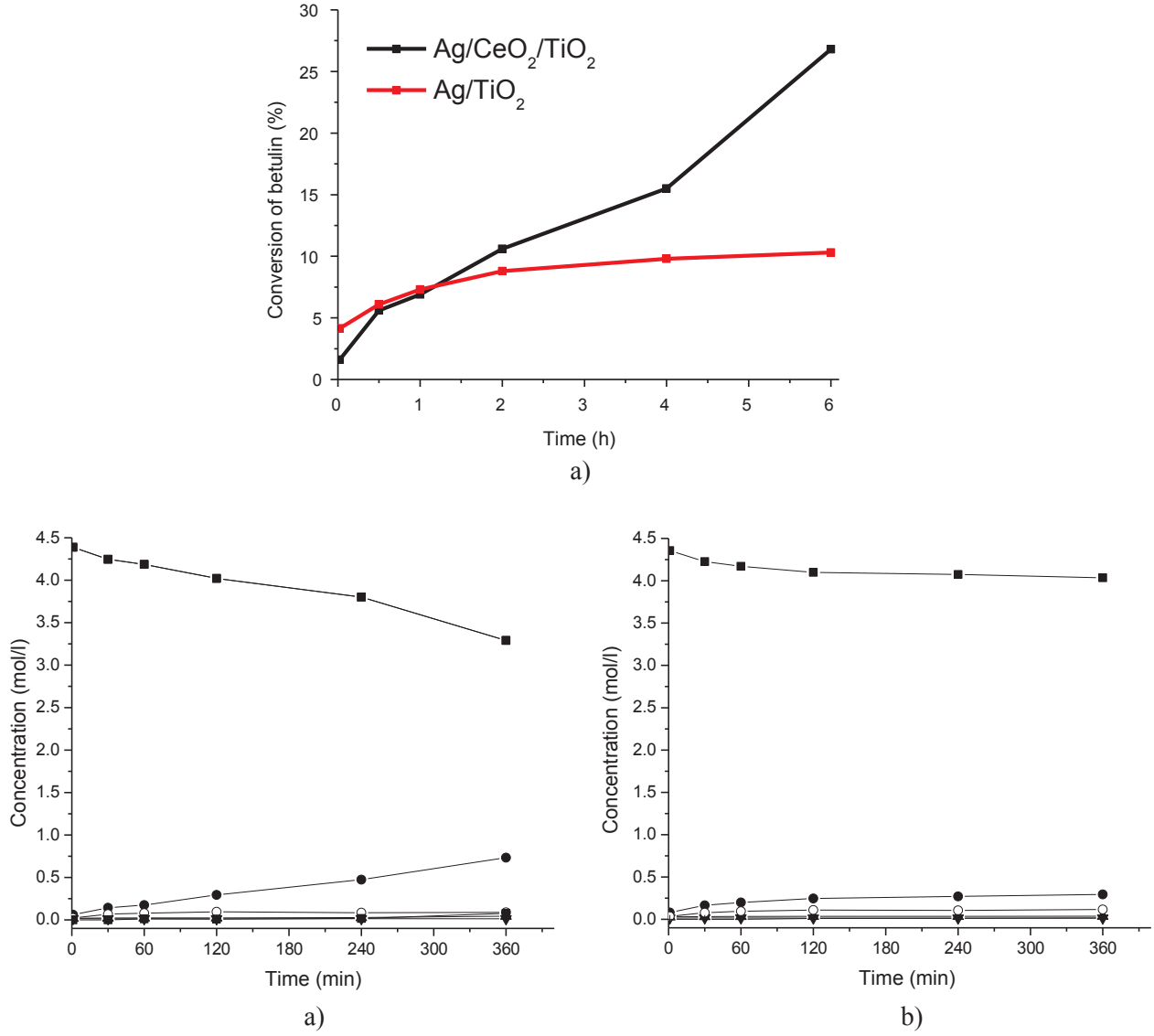

Fig. 2. Kinetics in betulin oxidation over supported as-prepared Ag catalysts. Selectivity of products of betulin oxidation for as-prepared $Ag/CeO_2/TiO_2$ (b) and Ag/TiO_2 (c) catalysts. Notation: (■) betulin, (●) betulone, (▲) betulonic aldehyde, (▼) betulonic acid, (o) betulinic aldehyde and (+) betulinic acid.

Table 1
Textural properties of the supports and catalysts, elemental composition and silver particle size (after pretreatment in H_2 at 300 °C for 1 h).

Samples	S_{BET} (m^2/g)		Ag content by EDX (wt%)	Metal particle size from HR TEM*	
	Support	Catalyst		Interval (nm)	Average (nm)
$Ag/CeO_2/TiO_2$	43	46	2.1 ± 0.4	3–12	7.2
$Ag/Fe_2O_3/TiO_2$	45	44	1.9 ± 0.4	1–2	1.1
$Ag/MgO/TiO_2$	42	43	2.0 ± 0.4	0–13	5.5
Ag/TiO_2	55	43	1.7 ± 0.3	Not detected	Not detected

* From[33].

samples have a size less than 1 nm [33]. The problem of the identification and characterization of subnanometer species undetectable by HRTEM was previously discussed in detail in [33]. On the contrary, silver particles were not detected in Ag/TiO_2 by HR TEM (Table 1), even if EDX confirms presence of silver. Probably silver is present in this sample in the form of surface compounds with the support, or in the form of very small clusters which have insufficient contrast to be detected by HRTEM.

H_2 TPR was used to study the essential features of silver reduction and to assess its electronic state in $Ag/M_xO_y/TiO_2$ catalysts, after *in-situ* pretreatment in oxidative (air) or reductive (10% vol. H_2/Ar) atmosphere at 300 °C (Fig. 3, Table 2). Several peaks of hydrogen consumption were observed in the high temperature region of the TPR profiles of the supports (Fig. 3). For TiO_2 (Fig. 3a) and MgO/TiO_2 (Fig. 3b), there is a slight increase of the background in the temperature range above 350 °C, which may be associated with partial reduction of TiO_2 [42,43]. For CeO_2/TiO_2 (Fig. 3d) the consumption from 372 to 473 °C is related to the reduction of surface cerium oxide with formation of Ce^{3+} states and oxygen vacancies; a temperature peak at 638 °C is related to reduction of bulk cerium oxide together with the reduction of Ce^{4+} to Ce^{3+} in the structure [44–50]. For Fe_2O_3/TiO_2 (Fig. 3c) the consumption peak at 334–457 °C is associated with the reduction of Fe_2O_3 to Fe_3O_4, and the one at 551 °C with reduction of Fe_3O_4 to FeO and further to Fe [51].

The most intense hydrogen consumption for more active catalysts

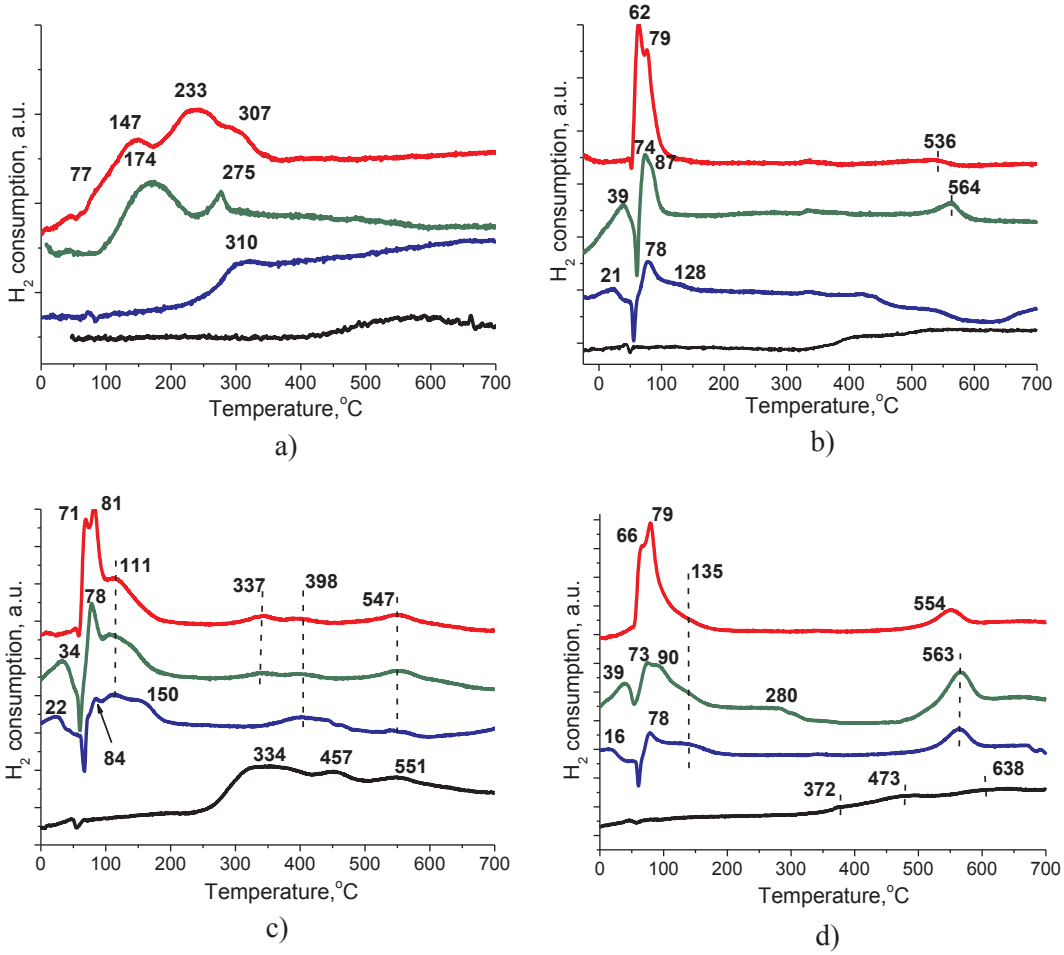

Fig. 3. TPR profile of as-prepared (red), pretreated in H_2 (blue), or air (olive) flow at 300 °C for 1 h Ag catalysts supported on initial TiO_2 (a) and on titania modified with Mg (b), Fe (c), Ce (d) oxides, their corresponding supports (black). (For interpretation of the references to colour in this figure legend, the reader is referred to the web version of this article.)

Table 2
Hydrogen consumption during TPR of catalysts as a function of their starting state: as-prepared, and pretreated in H_2 or in air.

Catalyst	Observed H_2 consumption (μmol/g_{cat})			Ag loading (μmol/g_{cat})
	as-prepared	H_2, 300 °C, 1 h	O_2, 300 °C, 1 h	
$Ag/CeO_2/TiO_2$	156	89	174	194 ± 39
$Ag/Fe_2O_3/TiO_2$	171	125	167	176 ± 35
$Ag/MgO/TiO_2$	77	40	72	185 ± 37
Ag/TiO_2	74	2	44	157 ± 31

(Fig. 3b, c, d) was observed in the temperature range 0–100 °C, associated with the reduction of oxide-like silver structures (surface silver oxides, highly dispersed silver oxides, small oxidized silver clusters, etc.) [52–54]. In the range 100–200 °C there was a co-reduction of silver and iron and cerium oxides (Fig. 3c, d) caused by their interactions [55,56]. The intensity of hydrogen consumption in the range of 50–100 °C, related to reduction of oxide-like structures of silver, decreased for samples pretreated in atmosphere of either O_2 or H_2, as compared to as-prepared samples. However, it should be noted that the active as-prepared samples consumed roughly the same amount of hydrogen before and after treatment in oxygen (Table 2). After pretreatment in hydrogen, the active samples were still able to consume some hydrogen; consequently, in the pretreatment conditions used (300 °C, 1 h), the reduction was incomplete. In addition, this effect may be due to the fact that silver ions in these samples are stable being less sensitive to redox treatments. A low temperature consumption at 77 °C, related to reduction of oxide-like structures of silver, is also observed in the TPR profile of Ag/TiO_2 (Fig. 3a); however, its intensity was significantly lower than for the active catalysts, explaining the observed catalytic behavior of this sample (Fig. 1a and Fig. 2a). Additional hydrogen consumption was observed for this material in the range of 150–400 °C, apparently due to reduction of surface compounds of silver with the support or reduction of silver oxide, strongly bound with the support.

After pretreatment in air, TPR profiles of all catalysts except Ag/TiO_2 showed consumption maxima in the range 0–50 °C, related to the reduction of silver oxide small clusters formed by oxidative dispersion of silver precursor [53,57], and at 547–554 °C. The latter can be explained by the reduction of strongly bound ionic silver from the surface compounds presumably of type Ti-O-Ag, similar to Si-O-Ag, which are reduced in the same temperature range [58]. This effect is most clearly visible for $Ag/CeO_2/TiO_2$.

The total amount of consumed hydrogen for Ag/TiO_2 and $Ag/MgO/TiO_2$ catalysts was close to ½ of amount of silver in catalysts (Table 2), which indicates that silver was stabilized in Ag+ state in the as-prepared samples. Higher values of consumed hydrogen for Ce- and Fe-containing samples are due to a partial reduction of iron and cerium oxides, respectively, together with that of silver oxide.

For all catalysts, the area of hydrogen consumption peaks in the temperature range 0–100 °C decreased after carrying out oxidation and

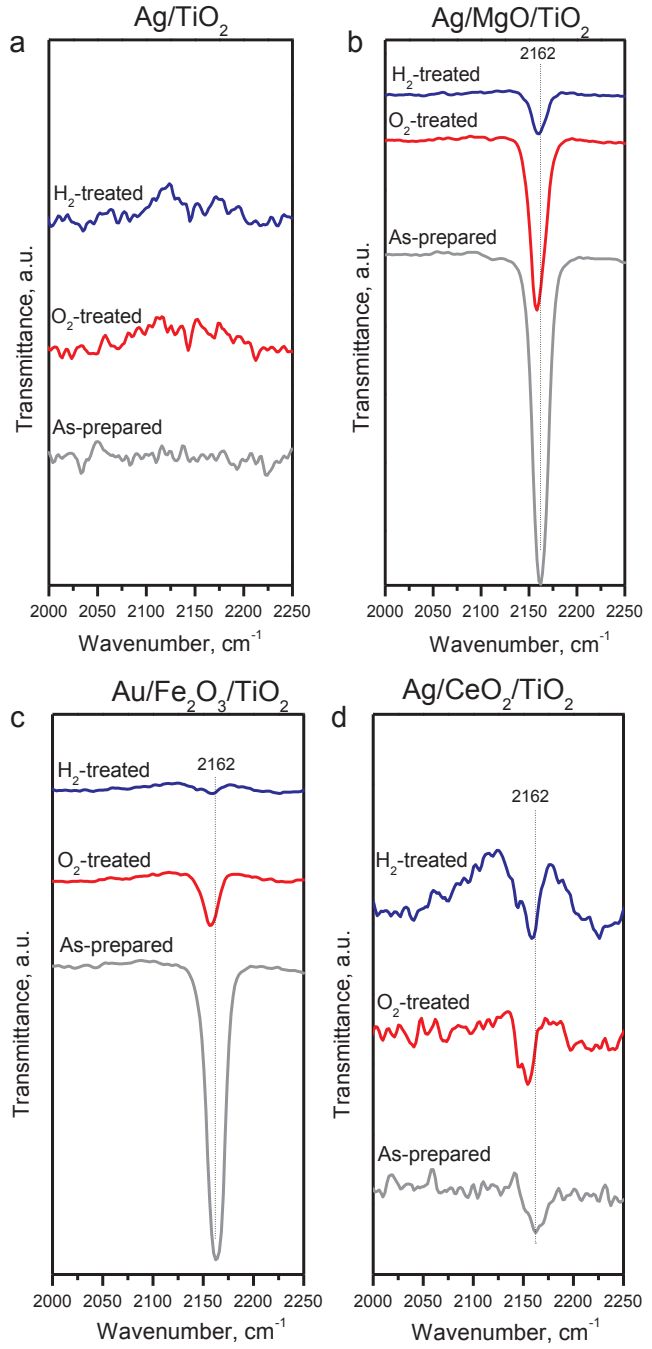

Fig. 4. Effect of catalyst pretreatment on the FTIR spectra of CO adsorbed on Ag/TiO_2 (a), $Ag/Mg/TiO_2$ (b), $Ag/Fe/TiO_2$ (c), $Ag/Ce/TiO_2$ (d).

reduction pretreatments, i.e., both oxidative and reductive thermal treatments led to a partial reduction of the samples. On the oxidizing atmosphere, this is due to thermal decomposition of unstable silver oxide (decomposition temperature is ca. 190 °C). A decrease in the amount of silver present in ionic/oxidized state in catalysts may be, apparently, a reason for activity decrease in n-octanol oxidation after such pretreatments (Fig. 1).

To investigate the electronic state of silver on the support surface, CO adsorption was studied by FTIR (Fig. 4). Absorption bands in the range 2150–2170 cm^{-1}, corresponding to linear carbonyls Ag^+-CO [59–67] were observed for $Ag/CeO_2/TiO_2$ (Fig. 3d), $Ag/Fe_2O_3/TiO_2$ (Fig. 4c) and $Ag/MgO/TiO_2$ (Fig. 4b) catalysts. The intensity of Ag^+-CO carbonyl absorption bands in the Ce-containing sample remained practically unchanged after redox pretreatmets (Fig. 4d). This suggests that the ionic species in this catalyst are stable and less sensitive to redox treatments. In contrast, for catalysts modified with magnesium and iron oxides (Fig. 4b and c) a significant decrease in the intensity of these absorption bands was observed after pretreatments. This indicates that ionic silver species are less stable in these samples. It might be that the initial amount of ionic sites in the as-prepared $Ag/MgO/TiO_2$ and $Ag/Fe_2O_3/TiO_2$ samples was higher than in $Ag/CeO_2/TiO_2$; however, these sites were less stable under the influence of the reaction medium, H_2 or O_2.

No absorption bands of Ag^+-CO carbonyls were observed in the IR spectra corresponding to Ag/TiO_2 (Fig. 4a), indicating absence of low-temperature adsorption centres. Noticeably, this catalyst shows the lowest activity in the studied processes (Fig. 1a and Fig. 2a). Probably, in this case only metastable silver active (ionic) sites are formed during the reaction due to interactions of oxygen with the metallic silver.

Based on the results presented above, it can be suggested that catalytic activity is determined by the contribution of Ag^+ sites which are retained after pretreatment and during catalysis.

XPS was used to study the electronic state of silver on the surface of unmodified and modified TiO_2 supports. It should be noted that prior to these tests the samples were pre-reduced in H_2 at 300 °C, and that reduction of silver may also take place under the influence of the X-ray beam; therefore, it should be expected that a part of silver is in the reduced state. Ag3d lines of XP spectra of all studied catalysts samples required deconvolution, as their half-width was much broader than the half-width corresponding to one state (Fig. 5). The interpretation of spectra, based on the literature, is shown in Table 3.

On the surface of Ce-, Fe- and Mg-containing catalysts silver is present in three states, with binding energy $E_b(Ag3d_{5/2})$ values of 366.6–366.8, 368.2 and 369.2–370.9 eV, respectively (Table 3). The first one corresponds to the ionic state of silver, Ag^+ [67,68], the second to the metal state, Ag^0 [33], while the latter is related to silver clusters smaller than 2 nm [69,70]. The binding energy of the latter species can be shifted, up to 1–2 eV, to higher values for highly dispersed metal particles deposited on oxide supports [71]. It should be noted that two states of silver with different binding energies corresponding to small silver clusters were observed in the XPS spectrum of the Mg-containing sample: probable reason for this may be different sizes of these clusters. On the surface of TiO_2 support (Fig. 5a) silver was present in two states with the binding energy E_b ($Ag3d_{5/2}$) = 367.5 eV, corresponding to the metal state, and 369.0 eV, corresponding to small silver clusters. These data are in good agreement with FTIR CO results (Fig. 4a) and TPR studies (Fig. 3a), showing that ionic silver is practically absent in this sample, and are apparently formed only during the reaction.

Thus, on the basis of the results of current work, it can be concluded that catalytic activity in n-octanol oxidation decreased with a decrease in the contribution of the surface silver monovalent state (shown respectively in the brackets): $Ag/CeO_2/TiO_2$ (57.2%) > $Ag/Fe_2O_3/TiO_2$ (15.1%) > $Ag/MgO/TiO_2$ (5.3%) > Ag/TiO_2 (0%).

It should be emphasized that one of the main problems in the study of M_xO_y/TiO_2 materials is differential charging of the surface during XPS measurements. To identify the effects associated with differential charging a modified Auger parameter α was applied, which represents the sum of binding energy values (Fig. 5) of the most intense line in the X-ray photoelectron spectrum of the studied element and the kinetic energy, which is consistent with the corresponding Auger peak [72]. Because the charge potential increases the binding energy of the internal level and diminishes the corresponding kinetic energy of the Auger peak to the same extent value, their sum with a charge change remains unaltered. Comparison of the parameter α calculated for Ag/TiO_2 (726.0 eV) and $Ag/CeO_2/TiO_2$ (724.1 eV), with the known values of α for metallic silver (726.0–726.3 eV) and silver oxide (724.0–724.5 eV) [72] indicates that the major fraction of silver is in the metallic state in Ag/TiO_2, while in $Ag/CeO_2/TiO_2$ s silver is in the ionic state, which is consistent with the results shown in Fig. 5a and d

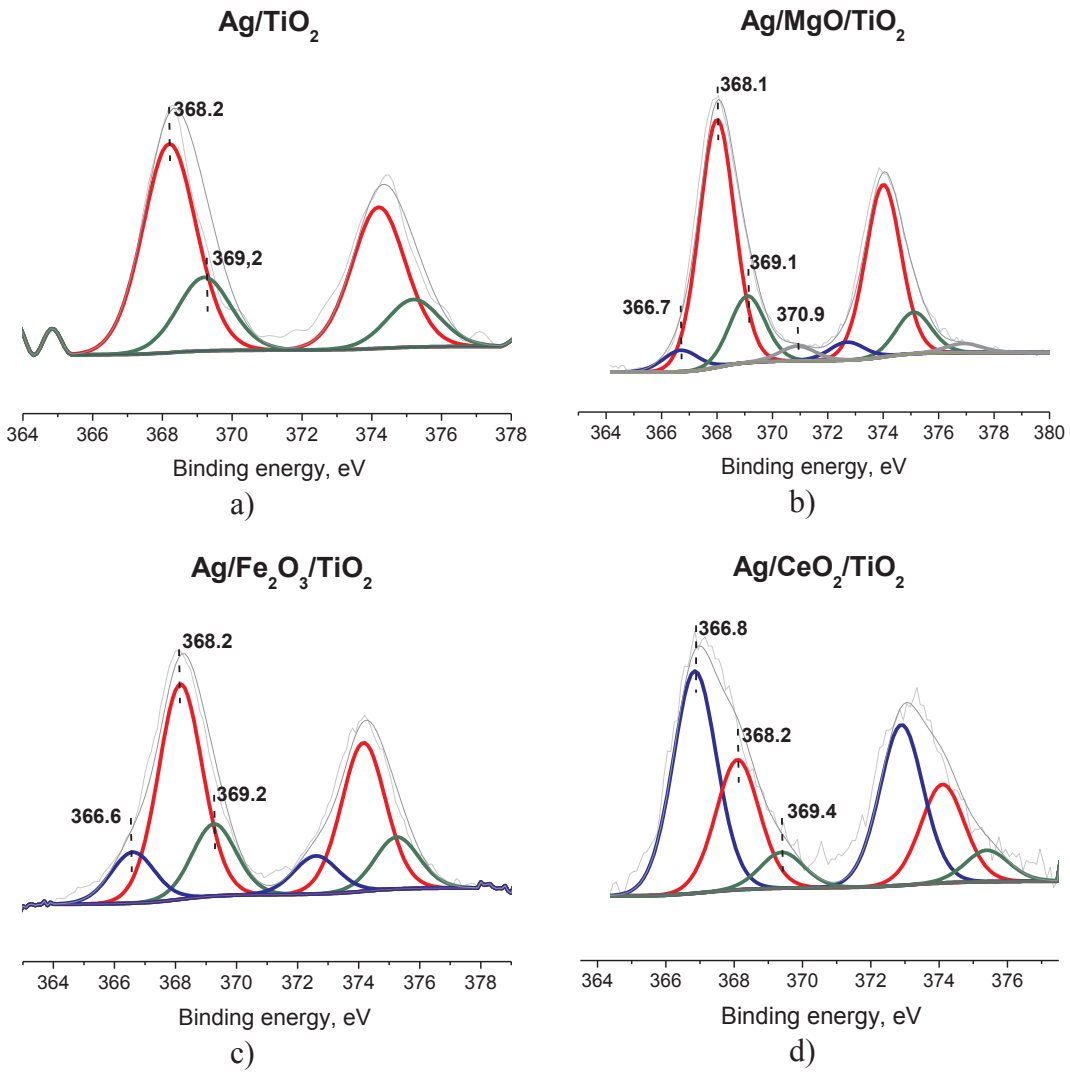

Fig. 5. XPS profiles of Ag $3d_{5/2}$ lines for Ag catalysts on different supports (TiO_2 (a), MgO/TiO_2 (b), Fe_2O_3/TiO_2 (c) and CeO_2/TiO_2 (d)) pretreated in H_2 at 300 °C for 1 h.

Table 3
XPS peaks assignments and content of silver states (%) in the catalysts after reduction in H_2 at 300 °C for 1 h.

Catalyst	Ag^+ (%)	Ag^0 (%)	Ag < 2 nm (%)
	366.6–366.8 eV [67,68]	368.0–368.2 eV [33]	≥369 eV [69–71]
$Ag/CeO_2/TiO_2$	57.2 (366.8 eV)	33.5 (368.2 eV)	9.3 (369.4 eV)
$Ag/Fe_2O_3/TiO_2$	15.1 (366.6 eV)	63.6 (368.2 eV)	21.3 (369.2 eV)
$Ag/MgO/TiO_2$	5.3 (366.7 eV)	61.2 (368.1 eV)	29.2 (369.1 eV) 4.3 (370.9 eV)
Ag/TiO_2	–	72.1 (368.2 eV)	27.9 (369.2 eV)

and Table 3. Furthermore, according to the literature [73,74], only metal crystallites with sizes ≥5 nm exhibit properties of the conductive metal. As the main fraction of silver particles for all studied samples has a size < 5 nm, the effect of the differential charging is unlikely.

Therefore, the main reason for the changes in the catalytic behaviour of $Ag/M_xO_y/TiO_2$ upon redox treatments and variation of the modifier nature is the change of the electronic state of silver. Comparison of TPR (Fig. 3) and FTIR CO spectroscopy data (Fig. 4) with the catalytic results (Fig. 1) suggests that catalytic activity in n-octanol oxidation after the redox treatments is associated with a decrease in the fraction of ionic/oxidized state of silver. The presence of the ionic state of silver for Ce, Fe and Mg-containing catalysts is confirmed by XPS spectroscopy (Fig. 5). On the basis of XPS data it was clearly shown above that catalytic activity decreased with a decrease in the surface concentration of the monovalent silver ions, which in turn, varies with the modifier nature. The highest concentration of the monovalent silver ions according to XPS data (Fig. 5d) was found in the cerium-modified material, and as a result, this catalyst showed the highest activity in both studied reactions. Ag/TiO_2 was the least active among the investigated catalysts. TPR (Fig. 3), FTIR CO (Fig. 4) and XPS (Fig. 5) results showed that the surface concentration of ionic species in this catalyst was minor, which probably is the main reason for its low catalytic activity. This is in line with the suggestion that the active sites are the monovalent silver ions. An important question is absence of the silver particles in TEM images, even if almost all silver in this catalyst is in the metallic state (XPS, Fig. 5a and FTIR CO, Fig. 4a). First a large fraction of silver particles is smaller than 1 nm, below the detection limit of TEM method. Second, formation of surface compounds of silver with the support is possible, which is confirmed by TPR (Fig. 3). Moreover, a combination of these two effects is possible, namely a large fraction of particles in this catalyst actually has a size lower than 1 nm, which may lead to very strong metal-support interactions and, as a consequence, formation of surface compounds of silver with the

support. Obviously, formation of the most active silver states requires some optimal interactions of the metal with the support, which stabilizes the ionic state of silver, but at the same time leaves them accessible for interactions with the reagents.

The main feature of the silver electronic state is stability of its d-orbitals and presence of a single stable ionic state – a mono charged Ag^+ cation (two- and three-charged silver ions are extremely unstable and exist only in the presence of strong oxidants). Therefore, the most effective promoters for silver are cerium oxide, which possess electron-accepting properties and stabilize active Ag^+ ions. In contrast, magnesium oxide has electron-donor properties that probably leads to reduction of a part of monovalent silver ions due to donation of electrons from magnesia to silver.

The results of current work showed that the introduction of the modifiers changes the nature of silver interactions with the support. This was confirmed by FTIR revealing interactions of active sites with the reagents (Ag^+-CO complexes, Fig. 4b, c, d), as well as presence of show the presence of a large number of silver nanoparticles in electronic micrographs [33]. Moreover, TPR data also showed a larger number of easily reducible silver ions in catalysts modified by Ce, Fe and Mg as compared with Ag/TiO_2 (Fig. 3). It can be hypothesized that the modifiers form a mixed oxide system with the support bearing new properties or alternatively silver in these samples is not deposited on the titania support surface, but on the modifier. A small particle size of the modifiers does not allow detecting their individual phases even by XRD and synchrotron radiation XRD, as previously shown in [33]. Thus, an exact nature of the modifier influence requires further investigations.

Comparison of catalytic results and physicochemical studies allows to conclude that in both reactions, 1-octanol and betulin oxidation, occur on similar active sites, individual Ag^+ ions or $Ag_n^{\delta+}$ clusters, where δ is in the range from 0 to 1. It should also be noted that the metallic phase is present in all the samples, however, correlation of its concentration with catalytic activity is not observed. Previously it was shown [75–77] that such metal states can be responsible for CO oxidation reaction, albeit at higher temperatures (above 100 °C).

It is important to note that in the literature there is no information about the activity of silver catalysts in these processes (oxidation of n-octanol and betulin), especially under conditions close to the requirements of green chemistry. The current work is the first study concerning the liquid-phase oxidation of n-octanol and betulin over modified and unmodified Ag/TiO_2 catalysts. The carried out researches show prospect of using silver-containing catalysts in the process of liquid-phase alcohols oxidation. However, several issues related to influence of various factors on activity, selectivity and stability of the studied catalysts should be solved to optimize the process and the catalyst: preparation methods, pretreatment conditions, nature of the support and the additives, active phase content, solvent type, temperature, substrates to catalyst ratio, presence of solid bases and dehydrating agents, etc.

4. Conclusions

The first time, silver supported on titania modified with Ce oxide were shown to be promising catalytic systems for liquid-phase oxidation of n-octanol and betulin under mild conditions adhering to the principles of green chemistry, e.g. atmospheric pressure, relatively low temperature (140 °C), O_2 or synthetic air as oxidants, and avoiding the use of alkali.

The main product of n-octanol oxidation, regardless of the nature of the modifying additives and the pretreatment atmosphere, is octanal (selectivity over 90% in all cases). Octanal is the most expensive and sought-after product of n-octanol oxidation. In the case of betulin oxidation, the main reaction product was betulone (> 60%). Betulone shows wound healing, anti-inflammatory and antitumor properties, and is also as a precursor of betululonic aldehyde and betulonic acid, which have more pronounced biologically active properties than it.

The active sites of $Ag/M_xO_y/TiO_2$ for the liquid phase oxidation of n-octanol and betulin are monovalent Ag^+ ions. The best promotional effect is observed after introduction of Ce oxide onto the support, while redox pretreatments are detrimental to catalytic activity due to a decrease in the surface concentration of monovalent ions. Strong interactions of silver with TiO_2 gives a uniform distribution of silver on the support surface, stabilizing it in the form of inactive surface compounds.

Nature of the support modifiers and pretreatment atmosphere influence the electronic state of the deposited metal, and thereby the catalytic properties.

The results also demonstrate potential of nanosilver catalysts for the liquid phase oxidation of alcohols, as their activity can be increased considerably by selecting the optimum modifier and the support as well as, pretreatment conditions.

Acknowledgements

The research is funded from Tomsk Polytechnic University Competitiveness Enhancement Program, project VIU-ISHBMT-196/2018; Russian Science Foundation project № 18-73-00019 (Russia); CONACYT project 279889 and PAPIIT-UNAM projects IT200114, IN105114 and IN107715 (Mexico); MINECO project CTQ2017-86170-R (Spain). The authors are grateful to Dr. O. Martynyuk, G. Torres Otañez, Z. I. Bedolla Valdez, Dr. E. Flores, F. Ruiz Medina, I. Gradilla, J. Mendoza, E.M. Aparicio Ceja, D.A. Domínguez, M. Martínez, J. Peralta, C. González Sanches and the Technical Support Unit of ICP for valuable technical assistance.

References

[1] Weissermel K, Arpe HJ. Industrial organic chemistry. 3rd ed. New York, NY: VCH; 1997.
[2] Cortés Corberán V, González-Pérez ME, Martínez-González S, Gómez-Avilés A. Green oxidation of fatty alcohols: challenges and opportunities. Appl Catal A Gen 2014;474:211–23. and references therein.
[3] Villa A, Dimitratos N, Chan-Thaw CE, Hammond C, Veith GM, Wang D, et al. Characterisation of gold catalysts. Chem Soc Rev 2016;45:4953–94.
[4] Megías-Sayago C, Ivanova S, López-Cartes C, Centeno MA, Odriozola JA. Gold catalysts screening in base-free aerobic oxidation of glucose to gluconic acid. Catal Today 2017;279:148–54.
[5] Kolobova E, Kotolevich Y, Pakrieva E, Mamontov G, Farías MH, Bogdanchikova N, et al. Causes of activation and deactivation of modified nanogold catalysts during prolonged storage and redox treatments. Molecules 2016;21(486):1–13.
[6] Wang J, Li Y, Peng Y, Song G. Silver nitrate-catalyzed selective air oxidation of benzylic and allylic alcohols to corresponding aldehydes or ketones. J Chin Chem Soc 2014;61:517–20.
[7] Nishiguchi T, Asano F. Oxidation of alcohols by metallic nitrates supported on silica gel. J Org Chem 1989;54:1531–5.
[8] Fetizon M, Golfier M. Selective oxidation of alcohols by silver carbonate. C R Acad Sci Ser C 1968;267:900–3.
[9] Balagh V, Fetizon M, Golfier M. Oxidations with silver carbonate/celite. Oxidations of phenols and related compounds. J Org Chem 1971;36:1339–41.
[10] Kakis FJ, Fetizon M, Douchkin N, Golfier M, Mourgues P, Prange T. Mechanistic studies regarding the oxidation of alcohols by silver carbonate on celite. J Org Chem 1974;39:523–33.
[11] Liotta LF, Venezia AM, Deganello G, Longo A, Martorana A, Schay Z, et al. Liquid phase selective oxidation of benzyl alcohol over Pd–Ag catalysts supported on pumice. Catal Today 2001;66:271–6.
[12] Adam F, Ahmed AE, Min SL. Silver modified porous silica from rice husk and its catalytic potential. J Porous Mater 2008;15:433–44.
[13] Nagaraju P, Balaraju M, Reddy KM, Sai Prasad PS, Lingaiah N. Selective oxidation of allylic alcohols catalyzed by silver exchanged molybdovanado phosphoric acid catalyst in the presence of molecular oxygen. Catal Commun 2008;9:1389–93.
[14] Mitsudome T, Mikami Y, Funai H, Mizugaki T, Jitsukawa K, Kaneda K. Oxidant-free alcohol dehydrogenation using a reusable hydrotalcite-supported silver nanoparticle catalyst. Angew Chem Int Ed 2008;47:138–41.
[15] Beier JM, Hansen TW, Grunwaldt J-D. Selective liquid phase oxidation of alcohols catalyzed by a silver-based catalyst in the presence of ceria. J Catal 2009;266:320–30.
[16] Shimizu K, Sugino K, Sawabe K, Satsuma A. Oxidant-free dehydrogenation of alcohols heterogeneously catalyzed by cooperation of silver clusters and acid–base sites on alumina. Chem Eur J 2009;15:2341–51.
[17] Shimizu K, Sawabe K, Satsuma A. Unique catalytic features of Ag nanoclusters for selective NO_x reduction and green chemical reactions. Catal Sci Technol

2011;1:331–41.
[18] Yadav GD, Yadav AR. Selective liquid phase oxidation of secondary alcohols into ketones by tert-butyl hydroperoxide on nano-fibrous Ag-OMS-2 catalyst. J Mol Catal A Chem 2013;380:70–7.
[19] Adil SF, Assal ME, Khan M, Al-Warthan A, Siddiqui MRH. Nano silver-doped manganese oxide as catalyst for oxidation of benzyl alcohol and its derivatives: synthesis, characterisation, thermal study and evaluation of catalytic properties. Oxid Commun 2013;36:778–91.
[20] Zahed B, Hosseini-Monfared H. A comparative study of silver-graphene oxide nanocomposites as arecyclable catalyst for the aerobic oxidation of benzyl alcohol: support effect. Appl Surf Sci 2015;328:536–47.
[21] Kotolevich Y, Kolobova E, Cabrera Ortega JE, Tiznado Vazquez HJ, Bogdanchikova N, Cortés Corberán V, Zanella R, Pestryakov A. Green n-octanol oxidation on promoted silver catalysts. Abst. 12th European congress on catalysis EuropaCat-XII, Kazan, Russia, 30 August – 4 September 2015. p. 1486–7.
[22] Van Santen R, Kuipers H. The mechanism of ethylene epoxidation. Adv Catal 1987;35:265–321.
[23] Dai WL, Cao Y, Ren LP, Yang XL, Xu JH, Li HX, et al. $AgSiO_2$–Al_2O_3 composite as highly active catalyst for the formation of formaldehyde from the partial oxidation of methanol. J Catal 2004;228:80–91.
[24] Lee JH, Schmieg SJ, Oh SH. Improved NO_x reduction over the staged Ag/Al_2O_3 catalyst system. Appl Catal A: Gen 2008;342:78–86.
[25] Zhang L, Zhang CB, He H. The role of silver species on Ag/Al_2O_3 catalysts for the selective catalytic oxidation of ammonia to nitrogen. J Catal 2009;261:101–9.
[26] Yamamoto R, Sawayama Y, Shibahara H, Ichihashi Y, Nishiyama S, Tsuruya S. Promoted partial oxidation activity of supported Ag catalysts in the gas-phase catalytic oxidation of benzyl alcohol. J Catal 2005;234:308–17.
[27] Nagy AJ, Mestl G, Schlögl R. The role of subsurface oxygen in the silver-catalyzed, oxidative coupling of methane. J Catal 1999;188:58–68.
[28] Purcar V, Donescu D, Petcu C, Luque R, Macquarrie DJ. Efficient preparation of silver nanoparticles supported on hybrid films and their activity in the oxidation of styrene under microwave irradiation. Appl Catal A Gen 2009;363:122–8.
[29] Magaev O, Knyazev A, Vodyankina O, Dorofeeva N, Salanov A, Boronin A. Active surface formation and catalytic activity of phosphorous-promoted electrolytic silver in the selective oxidation of ethylene glycol to glyoxal. Appl Catal A Gen 2008;344:142–9.
[30] Xu R, Wang X, Wang D, Zhou K, Li Y. Surface structure effects in nanocrystal MnO2 and Ag/MnO2 catalytic oxidation of CO. J Catal 2006;237:426–30.
[31] Liu H, Ma D, Blackley RA, Zhou W, Bao X. Highly active mesostructured silica hosted silver catalysts for CO oxidation using the one-pot synthesis approach. Chem Commun 2008:2677–9.
[32] Kolobova EN, Pestryakov AN, Shemeryankina AV, Kotolevich YS, Martynyuk OA, TiznadoVazquez HJ, et al. Formation of silver active states in Ag/ZSM-5 catalysts for CO oxidation. Fuel 2014;138:65–71.
[33] Kotolevich Y, Kolobova E, Khramov E, Cabrera JE, Farías MH, Zubavichus Y, et al. Cortés Corberán V. Molecules 2016;21:532–40.
[34] Sheldon RA. The E factor: fifteen years on. Green Chem 2007;9:1273–83.
[35] Wikholm N, Alakurtti S, Yli-Kauhaluoma J, Koskimies S. Method for preparation of betulinic acid; 2013, WO2013/038316 A1, Stora Enso Oyj, Helsinki, Finland.
[36] Tolstikov GA, Flekhter OB, Shultz EE, Baltina LA, Tolstikov AG. Betulin and its derivatives. Chemistry and biological activity. Chem Sus Dev 2005;13:1–29.
[37] Jonnalagadda SC, Suman P, Morgan DC, Seay JN. Recent developments on the synthesis and applications of betulin and betulinic acid derivatives as therapeutic agents. Stud Nat Prod Chem 2017;53:45–84. 117-xx.
[38] Muffler K, Leipold D, Scheller M-C, Haas C, Steingroewer J, Bley T, et al. Biotransformation of triterpenes. Process Biochem 2011;46:1–15.
[39] Mäki-Arvela P, Barsukova M, Winberg I, Smeds A, Hemming J, Eränen K, et al. Unprecedented selective heterogeneously catalysed “green” oxidation of betulin to biologically active compounds using synthetic air and supported Ru-catalysts. Chem Select 2016;1:3866–9.
[40] Eckerman C, Ekman R. Comparison of solvents for extraction and crystallization of betulinol from birch bark waste. Paperi ja Puu 1985;67:100–6.
[41] Melnikova N, Burlova I, Kiseleva T, Klabukova I, Gulenova M, Kislitsin A, et al. A practical synthesis of betulonic acid using selective oxidation of betulin on aluminium solid support. Molecules 2012;17:11849–63.
[42] Parida KM, Sahu N, Mohapatra P, Scurrell MS. Low temperature CO oxidation over gold supported mesoporous Fe–TiO_2. J Mol Cat A Chem 2010;319:92–7.
[43] Lenzi GG, Fávero CVB, Colpini LMS, Bernabe H, Baesso ML, Specchia S, Santos OAA. Photocatalytic reduction of Hg(II) on TiO_2 and Ag/TiO_2 prepared by the sol–gel and impregnation methods. Desalinations 2011;270:241–7.
[44] Yao HC, Yu YF. Ceria in automotive exhaust catalysts I. Oxygen storage. J Catal 1984;86:254–65.
[45] Zhu H, Qin Z, Shan W, Shen W, Wang J. Pd/CeO_2–TiO_2 catalyst for CO oxidation at low temperature: a TPR study with H_2 and CO as reducing agents. J Catal 2004;225:267–77.
[46] Jiang Y, Xing Z, Wang X, Huang S, Liu Q, Yang J. MoO_3 modified CeO_2/TiO_2 catalyst prepared by a single step sol–gel method for selective catalytic reduction of NO with NH_3. J Ind Eng Chem 2015;29:43–7.
[47] Wang L, Huang M, Li B, Dong L, Jin G, Gao J, et al. Enhanced hydrothermal stability and oxygen storage capacity of La^{3+} doped CeO_2-γ-Al_2O_3 intergrowth mixed oxides. Ceram Int 2015;41:12988–95.
[48] Wang H, Cao S, Fang Z, Yu F, Liu Y, Weng X, et al. CeO_2 doped anatase TiO_2 with exposed (001) high energy facets and its performance in selective catalytic reduction of NO by NH_3. Appl Surf Sci 2015;330:245–52.
[49] Kwon DW, Hong SC. Promotional effect of tungsten-doped CeO_2/TiO_2 for selective catalytic reduction of NO_x with ammonia. Appl Surf Sci 2015;356:181–90.
[50] Xu B, Zhang Q, Yuan S, Zhang M, Ohno T. Synthesis and photocatalytic performance of yttrium-doped CeO_2 with a porous broom-like hierarchical structure. Appl Catal B Environ 2016;183:361–70.
[51] Sepúlveda R, Plunk AA, Dunand DC. Microstructure of Fe_2O_3 scaffolds created by freeze-casting and sintering. Mat Lett 2015;142:56–9.
[52] Mamontov GV, Dutov VV, Sobolev VI, Vodyankina OV. Effect of transition metal oxide additives on the activity of an Ag/SiO_2 catalyst in carbon monoxide oxidation. Kinet Catal 2013;54:487–91.
[53] Qu Z, Huang W, Cheng M, Bao X. Restructuring and redispersion of silver on SiO_2 under oxidizing/reducing atmospheres and its activity toward CO oxidation. J Phys Chem B 2005;109:15842–8.
[54] Bondarchuk IS, Mamontov GV. Role of PdAg interface in Pd-Ag/SiO_2 bimetallic catalysts in low-temperature oxidation of carbon monoxide. Kinet Catal 2015;56:379–85.
[55] Liotta LF, Longo A, Macaluso A, Martorana A, Pantaleo G, Venezia AM, et al. Influence of the SMSI effect on the catalytic activity of a Pt(1%)/$Ce_{0.6}Zr_{0.4}O_2$ catalyst: SAXS, XRD, XPS and TPR investigations. Appl Catal B: Environ 2004;48:133–49.
[56] Kharlamova T, Mamontov G, Salaev M, Zaikovskii V, Popova G, Sobolev V, et al. Silica-supported silver catalysts modified by cerium/manganese oxides for total oxidation of formaldehyde. Appl Catal A Gen 2013;467:519–29.
[57] Dutov VV, Mamontov GV, Zaikovskii VI, Vodyankina OV. The effect of support pretreatment on activity of Ag/SiO_2 catalysts in low-temperature CO oxidation. Catal Today 2016;278:150–6.
[58] Mamontov GV, Izaak TI, Magaev OV, Knyazev AS, Vodyankina OV. Reversible oxidation/reduction of silver supported on silica aerogel: Influence of the addition of phosphate. Russ J Phys Chem A 2011;85:1536–41.
[59] Pestryakov A, Davydov A. Active electronic states of silver catalysts for methanol selective oxidation. Appl Catal A Gen 1994;120:7–15.
[60] Bechoux K, Marie O, Daturi M, Delahay G, Petitto C, Rousseau S, et al. Infrared evidence of room temperature dissociative adsorption of carbon monoxide over Ag/Al_2O_3. Catal Today 2012;197:155–61.
[61] Qiu Zh-Zh, Yu Y-X, Mi J-G. Adsorption of carbon monoxide on Ag(I)-ZSM-5 zeolite: An ab initio density functional theory study. Appl Surf Sci 2012;258:9629–35.
[62] Wichterlová B, Sazama P, Breen JP, Burch R, Hill CJ, Capek L, Sobalík Z. An in situ UV–vis and FTIR spectroscopy study of the effect of H_2 and. CO during the selective catalytic reduction of nitrogen oxides over a silver alumina catalyst. J. Catal 2005;235:195–200.
[63] Hadjiivanov KI. IR study of CO and NO_x sorption on Ag-ZSM-5. Micropor Mesopor Mater 1998;24:41–9.
[64] Hadjiivanov KI, Vayssilov GN. Characterization of oxide surfaces and zeolites by carbon monoxide as an IR probe molecule. Adv Catal 2002;47:307–511.
[65] Hadjiivanov KI, Knözinger H. Low-temperature CO adsorption on Ag^+/SiO_2 and Ag–ZSM-5: An FTIR study. J Phys Chem B 1998;102:10936–40.
[66] Jiang S, Huang S, Tu W, Zhu J. Infrared spectra and stability of CO and H_2O sorption over Ag-exchanged ZSM-5 zeolite: DFT study. Appl Surf Sci 2009;255:5764–9.
[67] Chang S, Li M, Hua Q, Zhang L, Ma Y, Ye B, et al. Shape-dependent interplay between oxygen vacancies and Ag–CeO_2 interaction in Ag/CeO_2 catalysts and their influence on the catalytic activity. J Catal 2012;293:195–204.
[68] Rtimi S, Baghriche O, Sanjines R, Pulgarin C, Bensimonc M, Kiwi J. TiON and TiON-Ag sputtered surfaces leading to bacterial inactivation under indoor actinic light. J Photochem Photobiol A 2013;256:52–63.
[69] Mejia MI, Marín M, Sanjines R. Pulgarín C., Mielczarski E., Mielczarski J., Kiwi L., Magnetron-sputtered Ag surfaces. New evidence for the nature of the Ag ions intervening in bacterial inactivation. ACS Appl. Mater. Interfaces 2010;2:230–5.
[70] López-Salido I, Lim DC, Kim YD. Ag nanoparticles on highly ordered pyrolytic graphite (HOPG) surfaces studied using STM and XPS. Surf Sci 2005;588:6–18.
[71] Mason MG. Electronic structure of supported small metal clusters. Phys Rev B 1983;27:748–62.
[72] Bukhtiyarov VI, Slin'ko MG. Metallic nanosystems in catalysis. Russ Chem Rev 2001;70(2):147–59.
[73] Barr TL. Studies in differential charging. J Vac Sci Technol A: Vac Surf Films 1989;7:1677–83.
[74] Barr TL. Advances in the application of X-ray photoelectron spectroscopy (ESCA). Part II. New methods. Crit Rev Anal Chem 1991;22:229–325.
[75] Pestryakov A, Tuzovskaya I, Smolentseva E, Bogdanchikova N, Jentoft F, Knop-Gericke A. Formation of gold nanoparticles in zeolites. Int J Modern Phys B 2005;19:2321–6.
[76] Pestryakov A, Bogdanchikova N, Simakov A, Tuzovskaya I, Jentoft F, Farias M, et al. Catalytically active gold clusters and nanoparticles for CO oxidation. Surf Sci 2007;601:3792–5.
[77] Smolentseva E, Bogdanchikova N, Simakov A, Pestryakov A, Avalos M, Farias MH, et al. Catalytic activity of gold nanoparticles incorporated into modified zeolites. J Nanosci Nanotechnol 2007;7:1882–6.